UDC 004.932:004.032.26:674.03

THE FRACTAL NEURAL NETWORK APPROACH FOR WOOD SPECIES CLASSIFICATION

Shymanskyi V. M. – PhD, Associate Professor, Department of Artificial Intelligence, Lviv Polytechnic National University, Lviv, Ukraine. ROR: https://ror.org/0542q3127. ORCID: https://orcid.org/0000-0002-7100-3263.

Shakhovska N. B. – Dr. Sc., Professor, Rector, Lviv Polytechnic National University, Lviv, Ukraine. ROR: https://ror.org/0542q3127. ORCID: https://orcid.org/0000-0002-6875-8534.

ABSTRACT

Context. Automated wood species recognition from macroscopic sections must combine high accuracy with stringent computational and memory requirements typical of peripheral devices and UAV onboard platforms. The heterogeneous, partially self-similar structure of wood texture, combining self-similar mid-level fluctuations with locally high-contrast elements and a large spread of leaders reflecting multifractality, motivates the creation of a fractal neural network architecture that can encode multiscale patterns while remaining computationally efficient.

Objective. The goal is to develop and validate fractal neural network models that achieve high recognition quality at reduced computational cost, enabling practical deployment on systems with limited resources.

Method. A fractal neural architecture (FractalNet) is employed to realize a self similar multi branch topology that forms an ensemble of receptive fields from fine to coarse scales, coherently modeling the spectrum of local regularities captured by leaders. The approach is benchmarked against ResNet50 and VGG16 with and without data augmentation on a 12 class macroscopic image task. Evaluation includes per class precision, recall, and F1, macro/weighted aggregates, confusion matrices, and analysis of numerical complexity in terms of trainable parameters and layer depth to assess deployability.

Results. The FractalNet combined with augmentation procedure attains the best overall performance, reaching macro F1 = 0.80, weighted F1 = 0.81, and accuracy = 0.81, outperforming ResNet50 (macro F1 = 0.57) and VGG16 (macro F1 = 0.71). Confusion matrices exhibit reduced cross class confusions, indicating more uniform gains across species. Despite superior accuracy, FractalNet contains ~0.37 M parameters versus 23.6 M in ResNet50 and 65.1 M in VGG16, yielding a markedly smaller memory footprint and lower inference latency.

Conclusions. The alignment between multifractal texture properties of wood and the self similar design of FractalNet produces a favorable accuracy-efficiency trade off. The method delivers state of the art recognition quality while preserving computational frugality, thus enabling reliable use in resource constrained scenarios, including UAV based and other edge deployments.

KEYWORDS: wood species recognition, fractal neural network, self similarity, data augmentation, UAV.

ABBREVIATIONS

AI is an artificial intelligence;

ANN is an artificial neural network;

CIFAR is a Canadian Institute for Advanced Research;

CNN is a convolutional neural network;

DWT is a discrete wavelet transform;

GAF is a gramian angular field;

GLCM is a gray level co-occurrence matrix;

Grad CAM is a gradient-weighted class activation mapping;

HSI is a hyperspectral imaging;

KDE is a kernel density estimate;

Layer CAM is a layer-wise class activation mapping;

LBP is a local binary patterns;

Micro CT is a micro-computed tomography;

NIR is a near-infrared;

PLS DA is a partial least squares discriminant analysis;

ResNet is a residual network;

SVM is a support vector machine;

THz is a terahertz;

UAV is an unmanned aerial vehicle;

VGG is a visual geometry group;

WTMM is a wavelet transform modulus maxima;

XRF is a x-ray fluorescence.

NOMENCLATURE

$A()$ is an operator from the set of affine transformations;

b is a bias;

BN is a batch normalization;

c is a class label;

D is a training set;

D_c is a set of examples of class c;

$d_{j,k}^{(s)}$ is a value of j-th, k-th feature of wavelet decomposition of the instance x_s;

$F()$ is a fractal-oriented neural network architecture;

F_{fl} is a a horizontal flip;

$f()$ is a quality functional;

f_{wev} is an operator of wavelet transformation;

K is a kernel;

$L_{j,k}$ is a j-th, k-th wavelet leader;

m is a largest number of instances;

n_c is a number of instances of class c;

$R(\varphi)$ is a rotation matrix by angle φ;

S_t is a subset of channels;

$Sh(\psi)$ is a shear matrix with angle ψ;

T is a number of channels;

DOI 10.15588/1607-3274-2026-2-11

$T_{tr}(o)$ is a translation to/from the image center o;

$Tr(h_x, h_y)$ is a shift on axes $x - h_x$, on axes $y - h_y$;

x_s is an instance s;

$x_{s,j,k}$ is a value of *j*-th, *k*-th input feature of the instance x_s;

x is a set of input instances;

x' is a set of validation input instances;

$\tilde{x}_s$ is an input vector with fractal descriptors;

$x_t^{(j)}$ is an output from the chanel S_t;

y is a set of output instances;

y' is a set of validation output instances;

$Z(z_x, z_y)$ is a nonisotropic scaling on axes $x - z_x$, on axes $y - z_y$;

λ is a regularization parameter;

$\lambda_{j,k}$ is a *j*-th, *k*-th cube;

ϕ is a nonlinear operator;

w is a set of controlled (adjusted) parameters of the neural network model;

$\Im_{cls}$ is a classification error operator;

$\Re()$ is a regularization operator;

$*$ is a convolution operator;

Φ_{fract} is a fractal transformation;

$\Im_{join}$ is a join operator;

$\hat{\lambda}_{loc}$ is a local aggregation operator;

$\hat{\lambda}_{glob}$ is a global aggregation operator.

INTRODUCTION

To automate decision-making processes in material control and object recognition tasks, it is necessary to have a model that characterizes the object or state of the material at the time of observation. In the field of wood identification, this is especially important, since fast and reliable species identification is critical for forest conservation, combating illegal logging, and ensuring the traceability of supply chains. Due to the lack or limitation of expert knowledge in practice, such models are mostly built on the basis of images, spectra, or other measurement data obtained in real conditions.

One of the most powerful tools for building models are artificial neural networks, in particular deep convolutional architectures, which have demonstrated high efficiency in species recognition tasks based on macroscopic sections, microanatomical structures, hyperspectral and NIR signals. Studies confirm that CNNs can automatically extract informative features of wood texture, achieving high accuracy for wide taxonomic sets.

The object of study is the process of recognizing wood species based on macroscopic sections.

The process of building such models is complex and computationally expensive, since the accuracy and speed of learning depend on the number, dimensionality and diversity of the sample and the architecture of the model. In the case of wood, this is complicated by the natural textural heterogeneity, variations in morphology and differences between data collection methods (images, spectra, microstructures). In such conditions, there is a pressing need to develop models that will provide high recognition accuracy while using relatively small computational costs. This will allow the use of such models on systems with limited computing resources, in particular UAVs.

The subject of study is the self-similar neural network models for automated recognition of wood species based on macroscopic sections.

In addition to classical texture descriptors, which are widely used for material analysis, fractal features are promising, which naturally describe the multi-scale heterogeneity of wood texture. It has been shown that the fractal dimension of pores and fibers correlates with the complexity of morphology and can enhance the quality of classification. Thus, self-similar neural network architectures open up the possibility of integrating fractal descriptors with deep neural models.

The purpose of the work is to develop self-similar neural network models that provide high accuracy in wood species recognition at reduced computational costs, which allows their effective application on systems with limited resources, in particular on UAV onboard computing platforms.

1 PROBLEM STATEMENT

Suppose given the original sample as a set of precedents (instances) $<x, y>$, where $x = \{x_s\}_{s=1}^{S}$, $x_s = \{x_{sj}\}_{j=1}^{N}$, $y = \{y_s\}_{s=1}^{S}$.

Each x_s instance correspond to one of the data sources relevant to the wood species classification task after unified preprocessing into a feature vector of dimension N.

To integrate multiscale texture information, we define a fractal transformation $\Phi_{fract}: R^N \to R^{N_j}$, which forms a vector of fractal descriptors. We assume that the input of the model is supplemented with these descriptors: $\tilde{x}_s = \left[x_s \middle\| \Phi_{fract}(x_s)\right] \in R^{N+N_j}$.

For a given set of instances $<x, y>$, the neural model synthesis problem is given as the pair finding problem $\langle F(\bullet), w\rangle$: $y_s = F(w, \tilde{x}_s)$, $f(F(\bullet), w, (x,y)) \to opt$. Where the model structure $F(\bullet)$ (fractal-oriented architecture) is specified by the researcher, and the controlled parameters w are adjusted based on the training set. The quality functional $f(\bullet)$ includes the classification error and regularizations penalties: $f = \Im_{cls}\left(\{(\tilde{x}_s, y_s)\}_{s=1}^{S}; F; w\right) + \lambda\Re(w)$.

DOI 10.15588/1607-3274-2026-2-11

In turn, the problem of subsample formation from a given sample $<x, y>$ is to find such a set of $<x', y'>$: $x' \subset \{x_s\}_{s=1}^{S}$, $y' = \{y_s | x_s \in x'\}$, wherein $f((x', y'), w, (x, y)) \to opt$.

Thus, within the framework of the article, a complex problem is solved of simultaneous:

1) synthesis of the architecture $F(\bullet)$ with fractal feature amplification;

2) finding the w parameters to take into account resource constraints;

3) formation of a representative subsample $<x', y'>$.

to minimize $f(\bullet)$ ensuring model applicability on systems with limited resources.

2 REVIEW OF THE LITERATURE

Rapid and reliable identification of wood species is critical for forest conservation, combating illegal logging, and ensuring proper certification of materials in supply chains. Over the past decade, AI-based methods have developed rapidly, including deep neural networks, which enable automatic species recognition from macroscopic and microanatomical images, hyperspectral/NIR data, and instrumental signals (XRF, Micro CT) [1].

A consistent line of research has been built around the application of CNN to macroscopic cross-section images: 90–96% accuracy for 15–281 species classes is achieved through transfer learning, resolution enhancement, and patch voting to capture fine textural patterns [2, 3].

CNNs are widely used for image classification in various fields, including medicine for image analysis and pathology detection [4–6], the automotive industry for computer vision systems in autonomous vehicles [7], security for face and object recognition [8, 9], industry for product quality control [10], and in entertainment technology for photo and video processing [11]. Their ability to automatically extract image features makes CNNs a key tool in modern artificial intelligence systems.

Deep learning for wood microsections operates on features of vessels, rays, parenchyma, which allows achieving accuracy >90% even for close taxa, when classical anatomical keys work mainly at the genus level. Importantly, recent work emphasizes explainability: Grad CAM/Layer CAM shows that networks focus on the same diagnostic patterns that experts use [12–14].

Hyperspectral and NIR data allow for non-destructive identification of rocks due to differences in light absorption and scattering. The "cognitive spectroscopy" approach, which gave 90.5% accuracy compared to 56% for conventional visible images, proved the informativeness of spectral data for rock recognition [15].

Portable NIR spectrometers with 1D spectra transformation into 2D matrix (GAF) and multi-scale CNN achieve high accuracy, which proves the suitability of the tool for field inspections and customs control practice. In addition, spectral pre-processing methods and cross-validation strategies were compared [16, 17].

For tropical wood species, high accuracy of PLS DA models on cubes obtained from chain and circular surface processing was also confirmed; while circular saw processing generates spectra that are more accurately classified [18]. Current approaches convert 1D NIR into 2D representations (Gramian Angular Field) and use multi-scale CNN, achieving ≈96% in validation [16]. Combining spectral modalities (NIR + HSI + THz) with feature extraction gives the best classification accuracy [19, 20].

Classical texture descriptors GLCM, LBP, Gabor filters are widely used in the classification of wood, defects, and related materials. LBP (rotation-invariant, uniform) variants are combined with SVM/ANN for defect recognition in wood and polywood [21–23]. Gabor filters and their optimization (Taguchi, genetic algorithms) improve the quality of wood texture and defect classification [24], [25]. Rotation invariance and high robustness have been proven for generalized texture recognition problems [26].

Fractal geometry offers a natural model for describing multiscale texture heterogeneity. Classical approaches use local/homogeneous fractal dimension and multifractal spectrum for segmentation and classification [27, 28]. For wood, it has been shown that the fractal dimension of the pore structure reflects the complexity of the morphology with comparable contributions from macro/micropores [29], and that the fractal dimension [30] can quantify the "graininess"/texture uniformity and assist in color matching [31].

FractalNet is a deep network architecture based on self-similarity with drop-path regularization, demonstrating ResNet-level performance on CIFAR/ImageNet without explicit residual connections [32]. For wood classification tasks, this opens up the possibility of combining fractal descriptors (as additional channels/pre-computed maps) with fractal macro-architectures, or incorporating multi-fractal features into CNNs. Recent work in related domains demonstrates that fractal networks have better generalizability to deep configurations, which is potentially useful for multi-scale wood textures [33, 34].

3 MATERIALS AND METHODS

The use of wavelet leaders for the analysis of wood cross-section images is theoretically justified within the framework of the multifractal formalism, which describes the local regularity of images through the Hölder exponents and their singular spectrum. In contrast to approaches that rely directly on wavelet coefficients or only on the modulus maxima lines (WTMM) [35], wavelet leaders form overscale "leaders" as supremums of local modulus coefficients in the scale pyramid in the immediate vicinity, thereby ensuring the correct reconstruction of the entire spectrum of singularities, including "oscillating" features, and not only its growing part [36].

For cross-sections of wood, where the texture is formed by the interaction of hierarchical structures (vessels, tracheids, annual rings, heart rays) with pronounced scale heterogeneity and anisotropy, wavelet

DOI 10.15588/1607-3274-2026-2-11

leaders are practically feasible: they provide stable estimates of multifractal attributes in 2D, better than the classical analysis of wavelet coefficients, and allow quantitatively describing the degree of self-similarity and variability of complexity at different spatial scales. It has been empirically shown that for images, the wavelet leader approach gives more accurate and stable estimates, which is critically important when comparing species, growth zones or detecting anomalies or defects in wood texture. In particular, for 2D data, the advantages of leaders over DWT coefficient methods have been demonstrated, which makes this approach a reliable tool for quantitative morphometry of natural textures.

2D wavelets are the standard basis for multifractal image analysis. The image is decomposed into 2D wavelets by the formula (1):

$$d_{j,k}^{(s)} = \left\langle f_{wev}, x_{s,j,k} \right\rangle. \quad (1)$$

For each scale j and position *k*, we calculate by the formula (2):

$$\left| d_{j,k} \right| = \max_i \left| d_{j,k}^{(s)} \right|. \quad (2)$$

A cube $\lambda_{j,k}$ is introduced and its extension by the formula (3):

$$3\lambda_{j,k} = \lambda_{j,k} \cup \{\text{neighbor cubes}\}. \quad (3)$$

The wavelet leader is defined as the maximum in the neighborhood among all smaller scales by the formula (4):

$$L_{j,k} = \sup_{\lambda' \subset 3\lambda_{j,k}} \left(\left| d_{j',k'} \right| : j' \le j \right), \quad (4)$$

That is, the leader is the "strongest" local oscillation of the image, taken over the entire scale hierarchy.

Leaders provide a complete correspondence between the Hölder exponent and the behavior of the wavelet coefficients, in contrast to the classical approach, which works only on a part of the spectrum.

This method is ideal for analyzing wood texture, as it has a pronounced hierarchy, is heterogeneous at different scales (vessels, fibers, annual rings), and contains both smooth and sharply oscillating structures.

To improve the efficiency of the training process of the developed model, a quantitative analysis of the dataset was conducted and a data balancing procedure was applied. The purpose of balancing is to equalize the number of examples in each class by stochastic augmentation of minority classes.

Let consider the training set $D = \{(x_s, y_s)\}_{s=1}^{N}$, where $x = \{x_s\}_{s=1}^{S}$ is an image, $y_i \in C = \{0,1,....S-1\}$ is a class.

For the class c, we denote the set of its examples $D_c = \{x_j : y_j = c\}$ and number of instances $n_c = |D_c|$. We will also determine the class with the largest number of instances $m = \max_c n_c$.

For each class c with $n_c < m$ new $m - n_c$ samples need to be generated. Each synthetic example is obtained as follows (5), (6):

$$x' = x \circ A(\theta)^{-1}, \quad (5)$$

$$A(\theta) = \{T(o); F(h); Z(z_x, z_y); Sh(\psi); R(\varphi); Tr(h_x, h_y)\}, \quad (6)$$

where $A(\theta)$ – operator from the set of affine transformations; $T_{tr}(o)$ – translation to/from the image center; $F_{fl}(h)$ – the horizontal flip; $Z(z_x, z_y)$ – nonisotropic scaling; $Sh(\psi)$ – shear matrix with angle ψ; $R(\varphi)$ – rotation matrix by angle φ; $Tr(h_x, h_y)$ – shift.

The main idea of the constructed self-similar neural network is that the network performs channel-wise feature evolution using a convolutional block, and then at each step averages a subset of active channels. Finally, global aggregation is performed. We force the channels to interact in various combinations, thereby enriching the representation, but at the same time leaving an inexpensive basic block in terms of parameters and a relatively easy fusion operation.

The convolutional block *conv_block* was chosen as the basic one, the functioning of which can be described by the formula (7)

$$conv\_block(x) = BN(\phi(K * x + b)), \quad (7)$$

where $x \in R^{H \times W \times C_{out}}$, $K \in R^{k \times k \times C_{in} \times C_{out}}$ – kernel, $b \in R^{C_{out}}$ – bias, ϕ – nonlinear operator, BN – batch normalization, $*$ – convolution.

At each step $t = 1,...,T$, a subset of channels is determined $S_t \subseteq \{0,...,C-1\}$

At each step, we "turn on" a certain subset of channels and allow them to mix through $\Im_{join}$. The remaining channels pass the step without mixing.

The channel update occurs according to the rule defined by formula (8):

$$\hat{x}_t^{(j)} = conv\_block\left(x_{t-1}^{(j)}\right). \quad (8)$$

For the activated subset S_t, a local merge is performed by formula (9):

$$\Im_{join}\left(\left\{\hat{x}_t^{(j)}\right\}_{j \in S_t}\right) = \frac{1}{|S_t|} \sum_{j \in S_t} \hat{x}_t^{(j)}. \quad (9)$$

DOI 10.15588/1607-3274-2026-2-11

Then the channel states are updated by the formula (10):

$$x_t^{(j)} = \begin{cases} \Im_{\text{join}}\left(\left\{\tilde{x}_t^{(p)}\right\}_{p\in S_t}\right) \\ x_{t-1}^{(j)} \end{cases}. \quad (10)$$

If more than one channel in S_t is enabled, they all receive the same mixed feature map. If there is only one channel in S_t, then it receives $x_{t-1}^{(j)}$.

Local aggregation by channels is implemented using formula (11).

$$\hat{\lambda}_{loc}\left(\left\{\tilde{x}_t^{(j)}\right\}_{j\in S_t}\right) = \frac{1}{\sum\limits_{j\in S_t} r_j}\sum_{j\in S_t} r_j \tilde{x}_t^{(j)}, \quad (11)$$

where $r_j \in \{0;1\}$, $j \in S_t$ – binary mask.

This mechanism allows to discard channels in the middle of a subset.

Global aggregation is implemented using formula (12)

$$\hat{\lambda}_{glob}\left(\left\{\tilde{x}_T^{(j)}\right\}_{j=0}^{C-1}\right) = \frac{1}{TC}\sum_{t=1}^{T}\sum_{j=0}^{C-1}\tilde{x}_t^{(j)}. \quad (12)$$

Thus, the choice of the wavelet leaders approach as the basis for multifractal analysis of wood cross-section images is justified and its practical applicability for 2D textures with pronounced hierarchy and anisotropy is shown. Unlike methods that work only with wavelet coefficients or maximum lines (WTMM), leaders capture the full spectrum of singularities. Such a formalization provides stable, reproducible estimates of self-similarity and variability at different spatial levels, which is critically important for quantitative morphometry of natural textures, comparison of species and growth zones. Complementing the analytical framework, the data preparation process is described for more efficient and stable model training. The dataset is balanced through stochastic augmentation of minority classes by affine transformations, which equalizes the frequencies of examples and reduces bias.

The proposed "self-similar" neural network performs per-channel feature evolution in a compact convolutional block with subsequent local mixing of activated subsets of channels, their updating by masks and global aggregation. Such an organization forces the channels to interact in various combinations and enriches the representation at a small parametric cost, organically combining with multifractal descriptors that provide wavelet leaders. Taken together, this forms a holistic, methodically verified pipeline – from the calculation of stable multi-scale features to their effective exploitation by the model – which forms the basis for further experiments and comparative analysis.

4 EXPERIMENTS

The experiments were designed to comprehensively evaluate the approach for multi-class classification of wood species from cross-section images [37, 38]. All images were standardized to a common spatial format and intensity range, and the spatial dimensions were aligned to a dyadic grid to enable a correct construction of the wavelet hierarchy. The training, validation, and test subsets were formed without overlap. Because of class imbalance, we applied dataset balancing via stochastic augmentation of minority classes: for each example, a random composition of affine transformations was generated (translation to/from the image center, horizontal flip, anisotropic scaling, shift, shear with a random angle, and rotations by moderate angles). The parameter ranges were chosen to preserve the morphological fidelity of natural wood texture (annual rings, vessels, tracheids, medullary rays) while keeping the statistics of fine-scale fluctuations – crucial for fractal analysis – unbiased.

Within a single pipeline, the presence of multifractal characteristics was analyzed using wavelet leaders. Images were decomposed on 2D wavelets; for each position and scale, a local neighborhood cube was constructed, and the leader was defined as the supremum of the absolute wavelet coefficients over all finer scales within that neighborhood. Based on this representation, we computed scaling moments, performed log-linear regressions within a stable scale range, and derived descriptors, and the width and shape of the singularity spectrum $f(\alpha)$.

The classifier architecture was implemented as a "self-similar" neural network, in which a baseline convolutional block performs channel-wise feature evolution; at each step, a random subset of channels is activated and mixed via the same convolution, while inactive channels bypass the step. For the activated subset, local merging is applied, followed by state updates using a binary mask; finally, global aggregation is performed. This organization deliberately encourages multi-way channel interactions across scales at a low parameter cost and is consistent with the hierarchical nature of wavelet leaders. Training was carried out on the balanced training set with simultaneous feeding of original or mildly augmented images. The loss function was cross-entropy; optimization used an adaptive gradient method with learning-rate decay; dropout regularization was additionally employed. Validity of estimates was ensured by a fixed train/val/test split. Performance was assessed by F1 and confusion matrices were analyzed for pairs of classes with similar morphology. To test statistical differences between models, paired nonparametric tests were used; significance was accepted at a conventional threshold.

The primary analysis showed that incorporating wavelet leaders substantially improves discrimination between classes with closely related textures, reducing confusions where conventional convolutional networks fail due to similar orientations and spatial frequencies. In the comparative study we considered: a CNN baseline without the self-similar block; and a ResNet with light fine-tuning.

DOI 10.15588/1607-3274-2026-2-11

The largest contribution to the F1 gain was provided by the self-similar channel-interaction mechanism, thanks to better aggregation of multiscale patterns with only a modest increase in parameters.

Analysis of the learning curves indicated stable convergence and lower validation loss for our model compared with the baselines. The confusion matrices demonstrated reduced cross-confusions between species pairs with subtle differences in vessel structure. Notably, the proposed model achieved high classification accuracy due to the effective integration of multifractal features and the self-similar channel-interaction mechanism, while remaining exceptionally compact: the number of trainable parameters was approximately two orders of magnitude lower than that of baseline deep architectures with comparable input sizes. This compactness not only reduces memory and training-time requirements but also increases robustness to overfitting on small and imbalanced image sets. Consequently, the model offers a superior quality – complexity trade-off and practical suitability for embedded or resource-constrained systems for automated wood-species identification.

Taken together, these results confirm that combining multifractal analysis with a self-similar neural network is an effective and robust solution for wood-species classification – especially in challenging cases with closely related textures – and that it surpasses baseline configurations on key metrics.

5 RESULTS

In the cross-section of wood, specific elements for each species are manifested in the size, density and grouping of vessels, the contrast of annual rings, pith rays, anisotropic structures with characteristic directions, transition zones and growth heterogeneity. Wavelet leaders specifically collect the strongest local oscillations across the entire scale hierarchy. Therefore, leader statistics are a compact indicator of how the texture behaves from small details to large structures. The Fig. 1 shows frequency histograms with a superimposed KDE curve for the distribution of the mean values of leaders (leaders_mean) (Fig. 1a) and the distribution of the standard deviations of leaders (leaders_std) (Fig. 1b), calculated for the test set of images, which were calculated using the method described by formulas (1)–(4). Analyzing the distribution of the mean values of leaders for each image, and then for the entire data set, allows you to analyze the unevenness of the image texture, the presence of self-similar oscillations. Analyzing this distribution of standard deviations of the leaders makes it possible to determine the presence of multifractal heterogeneity of the images.

Analysis of the dataset for balance is a fundamentally important stage in building a wood species classification system based on cross-sectional images, since the ratio of the number of examples between classes directly determines the statistical properties of the training sample, the nature of model optimization, and the correctness of the interpretation of the obtained metrics. The Fig. 2 shows the empirical distribution of the number of images by class in the training subsample before (Fig. 2a) and after (Fig. 2b) applying the balancing procedure by stochastic augmentation.

The mechanism for obtaining synthetic images, consists in randomly applying affine transformations to the original samples of minority classes, parameterized so as to preserve the semantic belonging to the species, but vary the permissible geometric manifestations of the texture. According to the given relations (5)–(6), the formation of each new example is carried out by a composition of operations of centering relative to the geometric center of the image, horizontal reflection, non-isotropic scaling, shear with angle ψ, rotation by angle α and spatial displacement. Centering and back translation play the role of a technical technique that ensures the correctness of rotation and scaling relative to the center of the frame, and not relative to the origin, due to which variations do not lead to a systematic “shift” of the structure beyond the field of view. The stochasticity of the choice of transformation parameters provides a variety of synthesized implementations, which increases intraclass variability without changing class semantics, and, as a result, makes the training distribution closer to the conditions of real shooting, where the orientation, scale and local positioning of the slice fragment may differ.

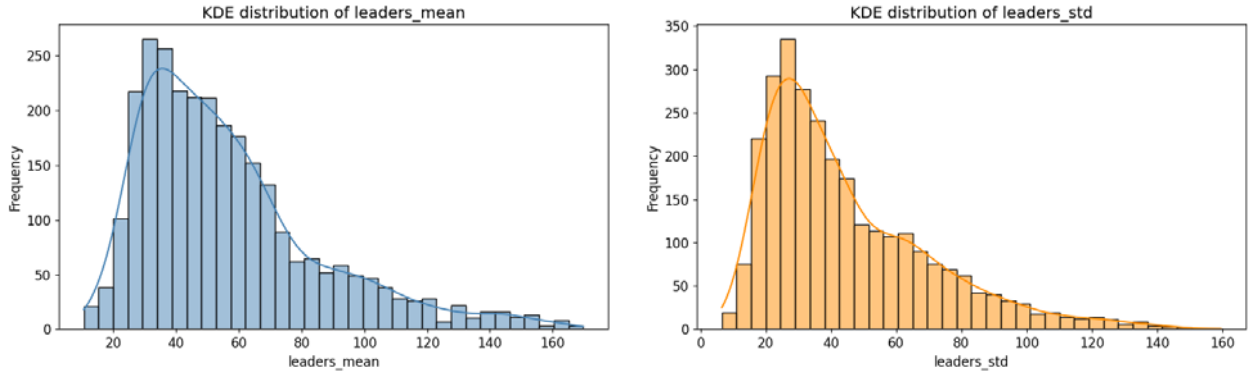

a b

Figure 1 – Frequency distribution histogram of leader for the test dataset:
a – leaders_mean; b – leaders_std

DOI 10.15588/1607-3274-2026-2-11

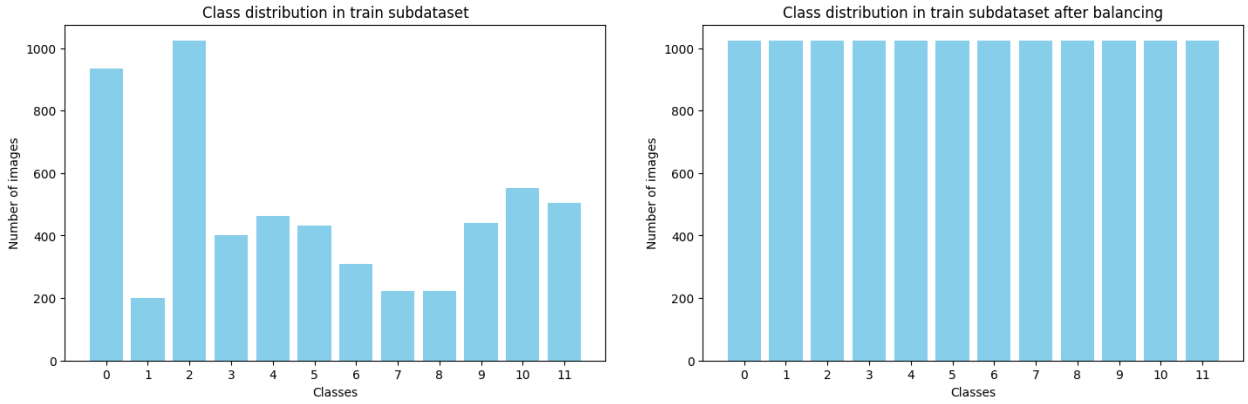

a b

Figure 2 – Class distribution in train subdataset:
a – in the training subdataset; b – in the balanced training subdataset

Thus, in terms of model training, after balancing, the contribution of each breed to the loss function becomes proportional, the dominance of the majority classes decreases, and the minority classes receive a sufficient number of variable examples for stable learning of the textural features of the cross section, which directly increases the expected generalizability of the classifier.

The Fig. 3 shows the visualization of the learning dynamics of the constructed self-similar neural network over 50 epochs on the training and validation subsamples. The left panel (Fig. 3a) displays the change in the value of the loss function, the right panel (Fig. 3b) – the change in the classification accuracy. Solid curves for training and validation allow us to assess not only the convergence rate of the optimization, but also the degree of generalization of the model and the presence of overtraining in the process of iterative parameter updating.

Obtaining these curves is directly related to the learning mechanism of the self-similar network. At each iteration, the model performs the evolution of features in the channels through the basic convolutional block, which implements the composition of convolution, normalization and nonlinearity according to (7), after which a subset of channels is activated at each step and local mixing and averaging of feature maps is performed for it according to the rules (8)–(11). At the output, global aggregation (12) is applied, which reduces the multichannel representation to a compact descriptor for the classification layer, after which the value of the loss function is calculated on the training set and the weights are updated using the gradient optimization method.

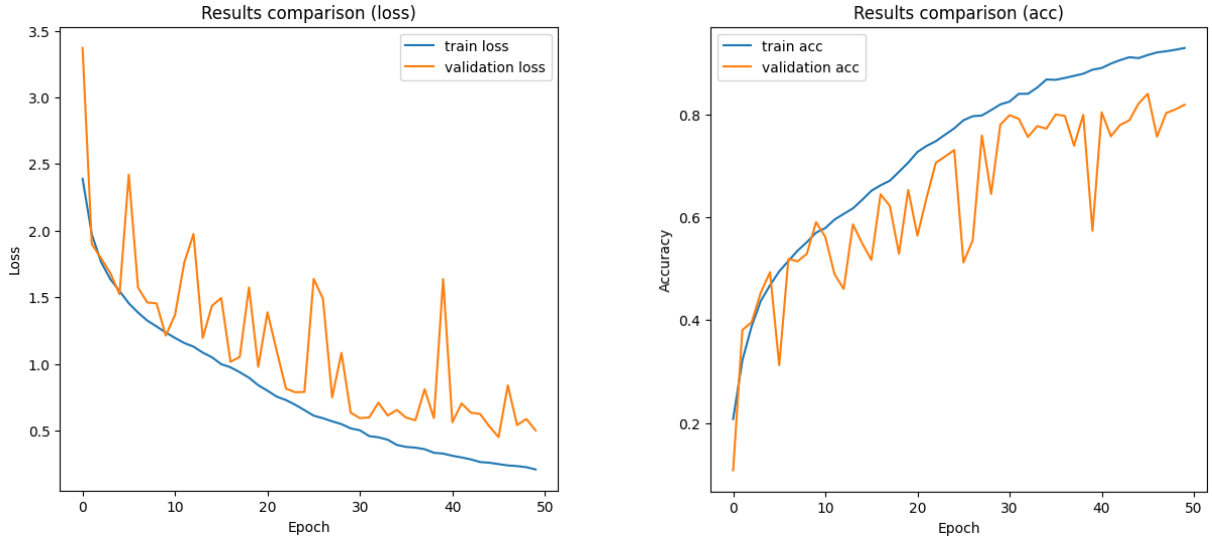

a b

Figure 3 – Training process visualization curves over epochs on the training and validation subsets:
a – loss; b – accuracy

DOI 10.15588/1607-3274-2026-2-11

Table 1 and Fig. 4 present the final results of multi-class classification of wood species from images. The dataset contained 12 classes (labels 0–11), the evaluation was carried out on an independent test set without using test examples during training. Four variants of the models were compared: ResNet50, VGG16, FractalNet with four fractal blocks and four columns without augmentation, as well as a similar FractalNet with augmentation. In all cases, the final classifier was set to a 12-class output with softmax. After training, the models were evaluated by basic quality indicators on the test: accuracy, as well as the Precision, Recall and F1 score metrics for each class, with subsequent aggregation into macro average and weighted average. A fragment of the numerical results is given in Table 1, and the nature of the errors and the distribution of predictions are illustrated by the confusion matrices in Fig. 4.

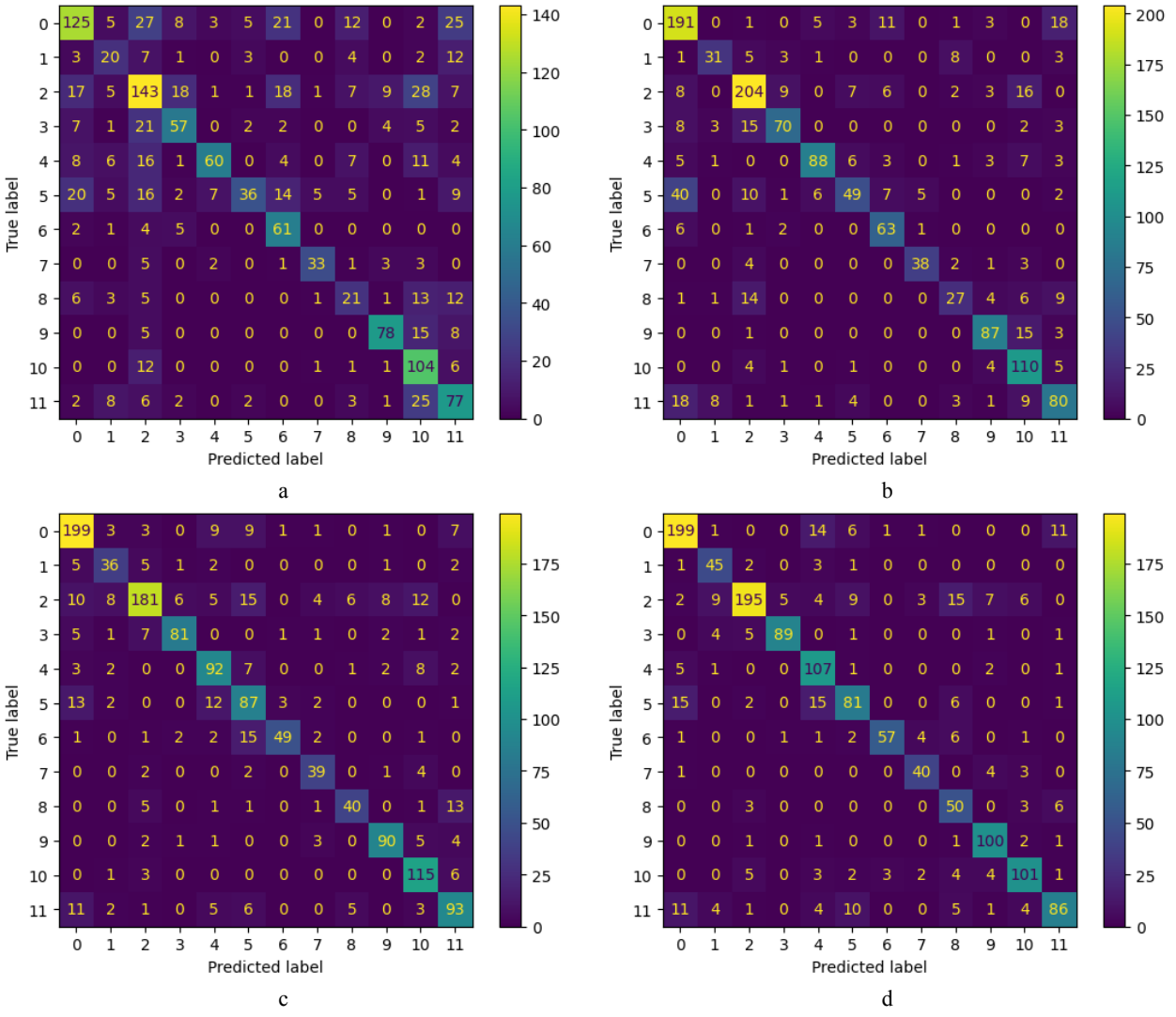

Figure 4 – Confusion matrices obtained during models evaluation:
a – ResNet50; b – VGG16; c – FractalNet (4 fractal blocks, 4 columns) without applying the augmentation procedure; d – FractalNet (4 fractal blocks, 4 columns) with applying the augmentation procedure

Analysis of confusion matrices (Fig. 4) and tabular metrics (Table1) is critically important because it allows us to evaluate not only the overall accuracy, but also the behavior of the model at the level of each class: to detect systematic confusion between specific breeds, to distinguish the impact of imbalance through the comparison of macro and weighted indicators, and to understand the trade-offs between Precision and Recall depending on the application requirements.

Table 2 presents quantitative characteristics of the three architectures used for wood species classification, namely the total number of parameters, the proportion of parameters that are learned, the amount of “frozen” parameters, and the number of layers.

DOI 10.15588/1607-3274-2026-2-11

Table 1 – Fragment of numerical results of models based on basic quality indicators

	Precision				Recall				F1-Score			
Metrics per model/class label	ResNet50	VGG 16	FractalNet without augmentation	FractalNet with augmentation	ResNet50	VGG16	FractalNet without augmentation	FractalNet with augmentation	ResNet50	VGG16	FractalNet without augmentation	FractalNet with augmentation
0	0.66	0.69	0.81	**0.85**	0.54	0.82	**0.85**	**0.85**	0.59	0.75	0.83	**0.85**
1	0.37	**0.70**	0.65	**0.70**	0.38	0.60	0.69	**0.87**	0.38	0.65	0.67	**0.78**
2	0.54	0.78	0.86	**0.91**	0.56	**0.80**	0.71	0.76	0.55	0.79	0.78	**0.83**
3	0.61	0.80	0.89	**0.94**	0.56	0.69	0.80	**0.88**	0.58	0.74	0.84	**0.91**
4	0.82	**0.87**	0.71	0.70	0.51	0.75	**0.79**	0.91	0.63	**0.81**	0.75	0.80
5	**0.73**	0.70	0.61	0.72	0.30	0.41	**0.72**	0.68	0.43	0.52	0.66	**0.70**
6	0.50	0.70	0.91	**0.93**	0.84	**0.86**	0.67	0.78	0.63	0.77	0.77	**0.85**
7	0.80	**0.86**	0.74	0.80	0.69	0.79	0.81	**0.83**	0.74	**0.83**	0.77	0.82
8	0.34	0.61	**0.77**	0.57	0.34	0.44	0.65	**0.81**	0.34	0.51	**0.70**	0.67
9	0.80	0.82	**0.86**	0.84	0.74	0.82	0.85	**0.94**	0.77	0.82	0.85	**0.89**
10	0.50	0.65	0.77	**0.84**	0.83	0.88	**0.92**	0.81	0.62	0.75	**0.84**	0.82
11	0.48	0.63	0.72	**0.80**	0.61	0.63	**0.74**	0.68	0.53	0.63	0.73	**0.74**
accuracy									0.57	0.73	0.78	**0.81**
macro avg	0.60	0.74	0.77	**0.80**	0.57	0.71	0.77	**0.82**	0.57	0.71	0.77	**0.80**
weighted avg	0.61	0.74	0.79	**0.82**	0.57	0.73	0.78	**0.81**	0.57	0.73	0.78	**0.81**

Table 2 – The fragment of the numerical characteristics of the model architecture

Model	Total params	Trainable params	Non-trainable params	Layers count
ResNet50	23.612.300	23.559.180	53.120	50
VGG16	65.103.692	65.103.692	0	16
FractalNet	365.196	362.700	2.496	140

The distinction between trainable and non-trainable reflects, in particular, the presence of layers such as convolutions with fixed normalization buffers or partially "frozen" components during fine-tuning, and the "Layers count" indicator characterizes the topological depth, which does not necessarily correlate with the amount of parameters, since the parameter collectivity is significantly affected by the width of the channels and the presence of large fully connected blocks.

6 DISCUSSION

The combination of self-similar mid-level oscillations with locally "hard" zones of high contrast and a large spread of leaders (Fig. 1), reflecting the multifractality of the texture, found in wood images, directly justifies the choice of fractal neural networks as an architecture with an appropriate inductive bias. Fractal topology implements a self-similar multi-branch organization of paths of different lengths and widths, due to which the network simultaneously forms an ensemble of receptive fields from fine to coarse scales and is able to coherently model the spectrum of local regularities that the leaders "see". At the feature level, this means that the same spatial regions can be represented by parallel branches, where shorter paths better encode sharp boundaries of annual rings, pores, cracks and other high-frequency elements, while longer paths accumulate low-frequency patterns of growth fibers and large-scale variations, providing resistance to irregularities and changes in contrast. As a result, the fractal network naturally approximates the multiscale spectrum of leaders, reduces cross-confusion between breeds where key differences manifest at different spatial scales, and increases the uniformity of quality between classes.

The numerical results in Table 1 demonstrate a consistent improvement in quality from ResNet50 to VGG16 and further to FractalNet, with the addition of augmentation to FractalNet providing additional gains. In terms of integral performance, the augmented FractalNet variant was the best: macro F1 increased from 0.57 in ResNet50 to 0.71 in VGG16, then to 0.77 in FractalNet without augmentation, and finally to 0.80 in FractalNet with augmentation; a similar trend is observed for weighted F1 (0.57 → 0.73 → 0.78 → 0.81). The accuracy indicator in the best configuration reaches 0.81, which is consistent with the increase in weighted metrics and reflects the improvement in more frequent classes. The increase in macro indicators indicates that the gain is not due only to the "dominant" classes, but is distributed more evenly between classes. Analysis of the results in Fig. 4 confirms the tabular findings. In ResNet50 (Fig. 4a), diagonal elements are less saturated, and off-diagonal cells have more noticeable values, which means a greater number of cross-confusions between classes. Switching to VGG16 (Fig. 4b) cleans the diagonal and reduces the number of errors, and FractalNet without augmentation (Fig. 4c) enhances this effect, providing an even more contrasting diagonal. The best result is observed in FractalNet with augmentation (Fig. 4d), since the diagonal values are the largest among all options, and the off-diagonal ones are the smallest, which is interpreted as the most stable recognition of each class. At the same time, different absolute values along the diagonal indicate uneven support of the classes in the test, so it is advisable to base the interpretation of the aggregated metrics on a combination of macro and weighted estimates, as presented in Table 1.

DOI 10.15588/1607-3274-2026-2-11

Comparison of Fig. 4 and Table1 allow us to draw an unambiguous conclusion about the advantage of multiscale fractal architecture in combination with data augmentation in the problem of wood species recognition. Reduction of cross-errors and systematic increase of both macro and weighted metrics mean better generalizability and more uniform quality of class prediction. In practice, this means that for production or laboratory scenarios where stability is important, the FractalNet configuration with augmentation is a reasonable starting point for further improvement.

An additional advantage is high parameter efficiency at high topological depth, which promotes generalizability without excessive memory footprint. Such models are easier to adapt for systems with limited resources, where low latency and economical memory usage are important, but at the same time the ability to take into account both smooth and sharp-contrast components of wood texture in real time is required. The combination of these properties – conformity to the self-similar nature of the data and computational frugality – makes fractal neural networks a feasible and technically justified choice for the problem of wood species classification.

CONCLUSIONS

The paper solves the urgent problem of building a highly accurate and at the same time computationally economical model of automated recognition of wood species from macroscopic sections. Within the framework of this problem, the use of self-similar (fractal) neural architectures is justified as solutions that are consistent with the heterogeneous and multifractal nature of wood texture and at the same time have low computational requirements, which makes them suitable for deployment on UAVs.

The scientific novelty lies in establishing a fundamental connection between the multifractal properties of wood images, the combination of self-similar oscillations of the average level with locally "rigid" high-contrast structures and a large spread of leaders, and the architecture of fractal neural networks that implement a self-similar multi-branch topology. Such a design makes it possible to model the spectrum of local regularities, thanks to which a systematic improvement is empirically achieved compared to classical convolutional basic models.

The practical significance of obtained results is twofold: first, the proposed fractal model achieves high accuracy with a significantly smaller number of model parameters, which directly reduces the memory footprint and inference latency; second, the achieved accuracy–efficiency balance allows it to work reliably on limited hardware without losing recognition capability, which facilitates implementation in field conditions of forest monitoring and in industrial quality control systems.

Prospects for further research lie in expanding the methodology to multimodal settings that combine macroscopic images with microanatomical or spectral data. Comprehensive testing on larger and more heterogeneous sets, taking into account different image acquisition protocols, will deepen the validity of the approach.

ACKNOWLEDGEMENTS

The study was performed without financial support.

DECLARATIONS

Conflict of interest: The authors declare that they have no conflict of interest in relation to this research, whether financial, personal, authorship, or otherwise, that could affect the research and its results presented in this paper.

Authors' contributions: Volodymyr Shymanskyi: data curation, investigation, methodology, resources, software, validation, visualization, writing – original draft; Nataliya Shakhovska: conceptualization, formal analysis, project administration, supervision, writing – review & editing.

Data availability: The manuscript has associated data in a data repository https://zenodo.org/records/2545611.

Software availability: The manuscript has no associated software.

Use of artificial intelligence tools: The authors confirm that they did not use artificial intelligence technologies in creating the submitted work.

REFERENCES

1. Yang X., Zheng Z., Zheng H., Liu X. Deep learning method of precious wood image classification based on microscopic computed tomography. *Russ J Nondestruct Test*, 2024, Vol. 60, № 10, pp. 1136–1148. DOI: 10.1134/S1061830924602447
2. He T., Mu S., Zhou H., Hu J. Wood species identification based on an ensemble of deep convolution neural networks. *WR,* 2021, Vol. 66, № 1, pp. 1–14. DOI: 10.37763/wr.1336-4561/66.1.0114
3. Wang C.-K., Zhao P. Classification of wood species using spectral and texture features of transverse section. *Eur. J. Wood Prod*, 2021, Vol. 79, № 5, pp. 1283–1296. DOI: 10.1007/s00107-021-01728-9
4. Berezsky O., Liashchynskyi P., Pitsun O., Izonin I. Synthesis of Convolutional Neural Network architectures for biomedical image classification. *Biomedical Signal Processing and Control,* 2024, Vol. 95, pp. 106325. DOI: 10.1016/j.bspc.2024.106325
5. Berezsky O. M., Liashchynskyi P. B., Pitsun O. Y., Melnyk G. M. Deep network-based method and software for small sample biomedical image generation and classification. *RIC,* 2024, № 4, P. 76. DOI: 10.15588/1607-3274-2023-4-8
6. Chapaliuk B. V., Zaychenko Y. P. Medical image segmentation methods overview. *SRIT,* 2018, Vol. 0, № 1, P. 72–81. DOI: 10.20535/SRIT.2308-8893.2018.1.05
7. Kim J. Deep learning-based vehicle type and color classification to support safe autonomous driving. *Applied Sciences,* 2024, Vol. 14, № 4, P. 1600. DOI: 10.3390/app14041600
8. Hu Z., Bodyanskiy Y. V., Kulishova N. Ye., Tyshchenko O. K. A multidimensional extended neo-fuzzy neuron for facial expression recognition. *IJISA,* 2017, Vol. 9, № 9, P. 29–36. DOI: 10.5815/ijisa.2017.09.04
9. Nemavhola A., Chibaya C., Viriri S. A systematic review of CNN architectures, databases, performance metrics, and ap-

DOI 10.15588/1607-3274-2026-2-11

plications in face recognition. *Information*, 2025, Vol. 16, № 2, P. 107. DOI: 10.3390/info16020107
10. Ke H. Using convolutional neural networks for material surface quality inspection and classification. *Int J Comput Intell Syst*, 2025, Vol. 18, № 1, P. 224. DOI: 10.1007/s44196-025-00951-z
11. Duvvuri K., Kanisettypalli H., Jaswanth K., Murali K.Video classification using CNN and ensemble learning. *9th International Conference on Advanced Computing and Communication Systems (ICACCS-2023), Coimbatore : proceedings, Coimbatore : IEEE*, 2023, pp. 66–70. DOI: 10.1109/ICACCS57279.2023.10112975
12. Zheng C. et al.Opening the black box: explainable deep-learning classification of wood microscopic image of endangered tree species. *Plant Methods*, 2024, Vol. 20, № 1, P. 56. DOI: 10.1186/s13007-024-01191-6
13. Liu S. et al.Automated species discrimination and feature visualization of closely related Pterocarpus wood species using deep learning models: comparison of four convolutional neural networks. *Wood Sci Technol*, 2025, Vol. 59, № 5, P. 86. DOI: 10.1007/s00226-025-01690-2
14. Kim T. K. et al. Identifying and extracting bark key features of 42 tree species using convolutional neural networks and class activation mapping. *Sci Rep*, 2022, Vol. 12, № 1, P. 4772. DOI: 10.1038/s41598-022-08571-9
15. Kanayama H., Ma T., Tsuchikawa S., Inagaki T. Cognitive spectroscopy for wood species identification: near infrared hyperspectral imaging combined with convolutional neural networks. *Analyst*, 2019, Vol. 144, № 21, pp. 6438–6446. DOI: 10.1039/C9AN01180C
16. Pan X., Yu Z., Yang Z. A multi-scale convolutional neural network combined with a portable near-infrared spectrometer for the rapid, non-destructive identification of wood species. *Forests*, 2024, Vol. 15, № 3, P. 556. DOI: 10.3390/f15030556
17. Park S.-Y. Kim J.-H., Kim J.-C., Yang S.-Y., Yeo H., Choi I.-G. Classification of softwoods using wood extract information and near infrared spectroscopy. *BioRes*, 2021, Vol. 16, № 3, pp. 5301–5312. DOI: 10.15376/biores.16.3.5301-5312
18. Novaes T. V. et al. Discrimination of Amazonian forest species by NIR spectroscopy: wood surface effects. *Eur. J. Wood Prod*, 2023, Vol. 81, № 1, P. 159–172. DOI: 10.1007/s00107-022-01862-y
19. He Y., Wang Y., Ma W. A multiple spectral important feature fusion method for wood species identification. *Wood Sci Technol*, 2025, Vol. 59, № 2, P. 34. DOI: 10.1007/s00226-025-01639-5
20. Li C., Wang Y. Optimizing recognition models for wood species identification using multi-spectral techniques. *Holzforschung*, 2025, Vol. 79, № 4–5, pp. 177–187. DOI: 10.1515/hf-2024-0112
21. Li S., Li D., Yuan W.Wood defect classification based on two-dimensional histogram constituted by LBP and local binary differential excitation pattern. *IEEE Access*, 2019, Vol. 7, pp. 145829–145842. DOI: 10.1109/ACCESS.2019.2945355
22. Rahiddin R. N. N., Hashim U. R., Ismail N. H., Salahuddin L., Choon N. H., Zabri S. N. Classification of wood defect images using local binary pattern variants. *Int. J. Adv. Intell. Informatics*, 2020, Vol. 6, № 1, P. 36. DOI: 10.26555/ijain.v6i1.392
23. Rahiddin R. N. N., Hashim U. R., Salahuddin L., Kanchymalay K., Wibawa A. P., Chun T. H. Local texture representation for timber defect recognition based on variation of LBP, *IJACSA*, 2022, Vol. 13, № 10. DOI: 10.14569/IJACSA.2022.0131053
24. Poelzleitner W., Schwingskakl G. Quality classification of wooden surfaces using Gabor filters and genetic feature optimization. *Photonics East '99 : proceedings*, Ed.: D. P. Casasent. Boston, 1999, pp. 220–231. DOI: 10.1117/12.360301
25. Yeh M.-F., Luo C.-C., Liu Y.-C. Optimization of Gabor convolutional networks using the Taguchi method and their application in wood defect detection. *Applied Sciences*, 2025, Vol. 15, № 17, P. 9557. DOI: 10.3390/app15179557
26. Porter R., Canagarajah N. Robust rotation-invariant texture classification: wavelet, Gabor filter and GMRF based schemes. *IEE Proc., Vis. Image Process*, 1997, Vol. 144, № 3, P. 180. DOI: 10.1049/ip-vis:19971182
27. Florindo J. B., Bruno O. M. Fractal descriptors based on Fourier spectrum applied to texture analysis, 2012. DOI: 10.48550/arXiv.1201.4597
28. Wang F., Li Z.-S., Liao G.-P.Multifractal detrended fluctuation analysis for image texture feature representation. *Int. J. Patt. Recogn. Artif. Intell*, 2014, Vol. 28, № 03, P. 1455005. DOI: 10.1142/S0218001414550052
29. Tibebu D. T., Avramidis S. Fractal dimension of wood pores from pore size distribution. *Holzforschung*, 2022, Vol. 76, № 11–12, P. 967–976. DOI: 10.1515/hf-2021-0175
30. Subbotin S. Methods of data sample metrics evaluation based on fractal dimension for computational intelligence model building. *4th International Scientific-Practical Conference Problems of Infocommunications. Science and Technology (PIC S&T), Kharkov : proceedings*. Kharkov, IEEE, 2017, pp. 1–6. DOI: 10.1109/INFOCOMMST.2017.8246136
31. He X. et al. Machine learning-based wood anatomy identification: towards anatomical feature recognition. *IAWA J*, 2024, Vol. 45, № 4, pp. 457–475. DOI: 10.1163/22941932-bja10157
32. Larsson G., Maire M., Shakhnarovich G. FractalNet: Ultra-deep neural networks without residuals. *arXiv*, 2016. DOI: 10.48550/ARXIV.1605.07648
33. Shymanskyi V., Ratinskiy O., Shakhovska N. Fractal neural network approach for analyzing satellite images. *Applied Artificial Intelligence*, 2025, Vol. 39, № 1, P. 2440839. DOI: 10.1080/08839514.2024.2440839
34. Shakhovska N., Shymanskyi V., Prymachenko M.FractalNet-LSTM model for time series forecasting. *CMC*, 2025, Vol. 82, № 3, pp. 4469–4484. DOI: 10.32604/cmc.2025.062675
35. Lin D. C., Sharif A. Wavelet transform modulus maxima based fractal correlation analysis, 2007. DOI: 10.1140/epjb/e2008-00004-6
36. Jaffard S., Lashermes B., Abry P. Wavelet leaders in multifractal analysis. *Wavelet Analysis and Applications : proceedings*, Eds.: T. Qian, M. I. Vai, Y. Xu. Basel, Birkhäuser Basel, 2007, pp. 201–246.
37. Barmpoutis P. Wood species dataset [Electronic resource]. Zenodo, 2019. DOI: 10.5281/ZENODO.2545611
38. Barmpoutis P., Dimitropoulos K., Barboutis I., Grammalidis N., Lefakis P. Wood species recognition through multidimensional texture analysis. *Computers and Electronics in Agriculture*, 2018, Vol. 144, pp. 241–248. DOI: 10.1016/j.compag.2017.12.011

Received 29.01.2026.
Accepted 20.04.2026.
Published 26.06.2026.

DOI 10.15588/1607-3274-2026-2-11

УДК 004.932:004.032.26:674.03

ФРАКТАЛЬНИЙ НЕЙРОМЕРЕЖЕВИЙ ПІДХІД ДЛЯ КЛАСИФІКАЦІЇ ПОРІД ДЕРЕВИНИ

Шиманський В. М. – канд. техн. наук, доцент, доцент кафедри систем штучного інтелекту Національного університету «Львівська політехніка», Львів, Україна. ROR: https://ror.org/0542q3127. ORCID: https://orcid.org/0000-0002-7100-3263.

Шаховська Н. Б. – д-р техн. наук, професор, ректор Національного університету «Львівська політехніка», Львів, Україна. ROR: https://ror.org/0542q3127. ORCID: https://orcid.org/0000-0002-6875-8534.

АНОТАЦІЯ

Актуальність. Автоматизоване розпізнавання видів деревини з макроскопічних зрізів повинно поєднувати високу точність зі строгими обчислювальними та пам'яттєвими характеристиками, типовими для периферійних пристроїв та бортових платформ БПЛА. Гетерогенна, частково самоподібна структура текстури деревини, що поєднує самоподібні коливання середнього рівня з локально висококонтрастними елементами та великим розкидом лідерів, що відображають мультифрактальність, мотивує створення фрактальної нейромережевої архітектури, яка зможе кодувати багатомасштабні закономірності, залишаючись при цьому ефективною за обчислювальними затратами.

Мета роботи полягає в розробці та валідації моделей фрактальних нейронних мереж, які досягають високої якості розпізнавання за знижених обчислювальних витрат, що дозволяє їх практичне застосування в системах з обмеженими ресурсами.

Метод. Для реалізації самоподібної багатогілкової топології, яка формує ансамбль рецептивних полів від дрібних до грубих масштабів, когерентно моделюючи спектр локальних закономірностей, що фіксуються лідерами, використовується фрактальна нейронна архітектура FractalNet. Підхід порівнюється з ResNet50 та VGG16 з доповненням даних та без нього на макроскопічному зображенні з 12 класами. Оцінювання включає точність, повноту та F1 для кожного класу, макро та зважені агрегати, матриці плутанини та аналіз числової складності з точки зору навчальних параметрів та глибини шарів для оцінки можливості застосування в системах з обмеженими ресурсами.

Результати. FractalNet у поєднанні з процедурою аугментації даних досягає найкращої загальної продуктивності, досягнувши macro F1=0,80, weighted F1=0,81 та точності = 0,81, перевершуючи ResNet50 (macro F1=0,57) та VGG16 (macro F1=0,71). Матриці плутанини демонструють зменшення міжкласової плутанини, що вказує на більш рівномірний приріст для різних видів. Незважаючи на вищу точність, FractalNet містить 0,37 млн параметрів порівняно з 23,6 млн у ResNet50 та 65,1 млн у VGG16, що призводить до значно меншого обсягу пам'яті та меншої затримки виведення.

Висновки. Узгодження мультифрактальних текстурних властивостей деревини та фрактальної архітектури FractalNet забезпечує вигідний компроміс між точністю та ефективністю. Метод забезпечує високу якість розпізнавання, зберігаючи при цьому обчислювальну ефективність, що дозволяє надійно використовувати його в системах з обмеженими ресурсами, включаючи розгортання на базі БПЛА та інших периферійних систем.

КЛЮЧОВІ СЛОВА: розпізнавання породи деревини, фрактальна нейронна мережа, самоподібність, доповнення даних, БПЛА.

ЛІТЕРАТУРА

1. Deep learning method of precious wood image classification based on microscopic computed tomography / [X. Yang, Z. Zheng, H. Zheng, X. Liu] // Russ J Nondestruct Test. – 2024. – Vol. 60, № 10. – P. 1136–1148. DOI: 10.1134/S1061830924602447
2. Wood species identification based on an ensemble of deep convolution neural networks / [T. He, S. Mu, H. Zhou, J. Hu] // WR. – 2021. – Vol. 66, № 1. – P. 1–14. DOI: 10.37763/wr.1336-4561/66.1.0114
3. Wang C.-K. Classification of wood species using spectral and texture features of transverse section / C.-K. Wang, P. Zhao // Eur. J. Wood Prod. – 2021. – Vol. 79, № 5. – P. 1283–1296. DOI: 10.1007/s00107-021-01728-9
4. Synthesis of Convolutional Neural Network architectures for biomedical image classification / [O. Berezsky, P. Liashchynskyi, O. Pitsun, I. Izonin] // Biomedical Signal Processing and Control. – 2024. – Vol. 95. – P. 106325. DOI: 10.1016/j.bspc.2024.106325
5. Deep network-based method and software for small sample biomedical image generation and classification / [O. M. Berezsky, P. B. Liashchynskyi, O. Y. Pitsun, G. M. Melnyk] // RIC. – 2024. – № 4. – P. 76. DOI: 10.15588/1607-3274-2023-4-8
6. Chapaliuk B. V. Medical image segmentation methods overview / B. V. Chapaliuk, Y. P. Zaychenko // SRIT. – 2018. – Vol. 0, № 1. – P. 72–81. DOI: 10.20535/SRIT.2308-8893.2018.1.05
7. Kim J. Deep learning-based vehicle type and color classification to support safe autonomous driving / J. Kim // Applied Sciences. – 2024. – Vol. 14, № 4. – P. 1600. DOI: 10.3390/app14041600
8. A multidimensional extended neo-fuzzy neuron for facial expression recognition / [Z. Hu, Y. V. Bodyanskiy, N. Ye. Kulishova, O. K. Tyshchenko] // IJISA. – 2017. – Vol. 9, № 9. – P. 29–36. DOI: 10.5815/ijisa.2017.09.04
9. Nemavhola A. A systematic review of CNN architectures, databases, performance metrics, and applications in face recognition / A. Nemavhola, C. Chibaya, S. Viriri // Information. – 2025. – Vol. 16, № 2. – P. 107. DOI: 10.3390/info16020107
10. Ke H. Using convolutional neural networks for material surface quality inspection and classification / H. Ke // Int J Comput Intell Syst. – 2025. – Vol. 18, № 1. – P. 224. DOI: 10.1007/s44196-025-00951-z
11. Video classification using CNN and ensemble learning / [K. Duvvuri, H. Kanisettypalli, K. Jaswanth, K. Murali] // 9th International Conference on Advanced Computing and Communication Systems (ICACCS-2023), Coimbatore : proceedings. – Coimbatore : IEEE, 2023. – P. 66–70. DOI: 10.1109/ICACCS57279.2023.10112975
12. Opening the black box: explainable deep-learning classification of wood microscopic image of endangered tree species / C. Zheng et al. // Plant Methods. – 2024. – Vol. 20, № 1. – P. 56. DOI: 10.1186/s13007-024-01191-6

DOI 10.15588/1607-3274-2026-2-11

13. Automated species discrimination and feature visualization of closely related Pterocarpus wood species using deep learning models: comparison of four convolutional neural networks / S. Liu et al. // Wood Sci Technol. – 2025. – Vol. 59, № 5. – P. 86. DOI: 10.1007/s00226-025-01690-2
14. Identifying and extracting bark key features of 42 tree species using convolutional neural networks and class activation mapping / T. K. Kim et al. // Sci Rep. – 2022. – Vol. 12, № 1. – P. 4772. DOI: 10.1038/s41598-022-08571-9
15. Cognitive spectroscopy for wood species identification: near infrared hyperspectral imaging combined with convolutional neural networks / [H. Kanayama, T. Ma, S. Tsuchikawa, T. Inagaki] // Analyst. – 2019. – Vol. 144, № 21. – P. 6438–6446. DOI: 10.1039/C9AN01180C
16. Pan X. A multi-scale convolutional neural network combined with a portable near-infrared spectrometer for the rapid, non-destructive identification of wood species / X. Pan, Z. Yu, Z. Yang // Forests. – 2024. – Vol. 15, № 3. – P. 556. DOI: 10.3390/f15030556
17. Classification of softwoods using wood extract information and near infrared spectroscopy / [S.-Y. Park, J.-H. Kim, J.-C. Kim et al.] // BioRes. – 2021. – Vol. 16, № 3. – P. 5301–5312. DOI: 10.15376/biores.16.3.5301-5312
18. Novaes T. V. Discrimination of Amazonian forest species by NIR spectroscopy: wood surface effects / T. V. Novaes, et al. // Eur. J. Wood Prod. – 2023. – Vol. 81, № 1. – P. 159–172. DOI: 10.1007/s00107-022-01862-y
19. He Y. A multiple spectral important feature fusion method for wood species identification / Y. He, Y. Wang, W. Ma // Wood Sci Technol. – 2025. – Vol. 59, № 2. – P. 34. DOI: 10.1007/s00226-025-01639-5
20. Li C. Optimizing recognition models for wood species identification using multi-spectral techniques / C. Li, Y. Wang // Holzforschung. – 2025. – Vol. 79, № 4–5. – P. 177–187. DOI: 10.1515/hf-2024-0112
21. Li S. Wood defect classification based on two-dimensional histogram constituted by LBP and local binary differential excitation pattern / S. Li, D. Li, W. Yuan // IEEE Access. – 2019. – Vol. 7. – P. 145829–145842. DOI: 10.1109/ACCESS.2019.2945355
22. Classification of wood defect images using local binary pattern variants / [R. N. N. Rahiddin, U. R. Hashim, N. H. Ismail et al.] // Int. J. Adv. Intell. Informatics. – 2020. – Vol. 6, № 1. – P. 36. DOI: 10.26555/ijain.v6i1.392
23. Local texture representation for timber defect recognition based on variation of LBP / [R. N. N. Rahiddin, U. R. Hashim, L. Salahuddin et al.] // IJACSA. – 2022. – Vol. 13, № 10. DOI: 10.14569/IJACSA.2022.0131053
24. Poelzleitner W. Quality classification of wooden surfaces using Gabor filters and genetic feature optimization / W. Poelzleitner, G. Schwingskakl // Photonics East '99 : proceedings / Ed.: D. P. Casasent. – Boston, 1999. – P. 220–231. DOI: 10.1117/12.360301
25. Yeh M.-F. Optimization of Gabor convolutional networks using the Taguchi method and their application in wood defect detection / M.-F. Yeh, C.-C. Luo, Y.-C. Liu // Applied Sciences. – 2025. – Vol. 15, № 17. – P. 9557. DOI: 10.3390/app15179557
26. Porter R. Robust rotation-invariant texture classification: wavelet, Gabor filter and GMRF based schemes / R. Porter, N. Canagarajah // IEE Proc., Vis. Image Process. – 1997. – Vol. 144, № 3. – P. 180. DOI: 10.1049/ip-vis:19971182
27. Florindo J. B. Fractal descriptors based on Fourier spectrum applied to texture analysis / J. B. Florindo, O. M. Bruno. – 2012. DOI: 10.48550/arXiv.1201.4597
28. Wang F. Multifractal detrended fluctuation analysis for image texture feature representation / F. Wang, Z.-S. Li, G.-P. Liao // Int. J. Patt. Recogn. Artif. Intell. – 2014. – Vol. 28, № 03. – P. 1455005. DOI: 10.1142/S0218001414550052
29. Tibebu D. T. Fractal dimension of wood pores from pore size distribution / D. T. Tibebu, S. Avramidis // Holzforschung. – 2022. – Vol. 76, № 11–12. – P. 967–976. DOI: 10.1515/hf-2021-0175
30. Subbotin S. Methods of data sample metrics evaluation based on fractal dimension for computational intelligence model building / S. Subbotin // 4th International Scientific-Practical Conference Problems of Infocommunications. Science and Technology (PIC S&T), Kharkov : proceedings. – Kharkov : IEEE, 2017. – P. 1–6. DOI: 10.1109/INFOCOMMST.2017.8246136
31. Machine learning-based wood anatomy identification: towards anatomical feature recognition / X. He et al. // IAWA J. – 2024. – Vol. 45, № 4. – P. 457–475. DOI: 10.1163/22941932-bja10157
32. Larsson G. FractalNet: Ultra-deep neural networks without residuals / G. Larsson, M. Maire, G. Shakhnarovich // arXiv. – 2016. DOI: 10.48550/ARXIV.1605.07648
33. Shymanskyi V. Fractal neural network approach for analyzing satellite images / V. Shymanskyi, O. Ratinskiy, N. Shakhovska // Applied Artificial Intelligence. – 2025. – Vol. 39, № 1. – P. 2440839. DOI: 10.1080/08839514.2024.2440839
34. Shakhovska N. FractalNet-LSTM model for time series forecasting / N. Shakhovska, V. Shymanskyi, M. Prymachenko // CMC. – 2025. – Vol. 82, № 3. – P. 4469–4484. DOI: 10.32604/cmc.2025.062675
35. Lin D. C. Wavelet transform modulus maxima based fractal correlation analysis / D. C. Lin, A. Sharif. – 2007. DOI: 10.1140/epjb/e2008-00004-6
36. Jaffard S. Wavelet leaders in multifractal analysis / S. Jaffard, B. Lashermes, P. Abry // Wavelet Analysis and Applications : proceedings / Eds.: T. Qian, M. I. Vai, Y. Xu. – Basel : Birkhäuser Basel, 2007. – P. 201–246.
37. Barmpoutis P. Wood species dataset [Electronic resource]. – Zenodo, 2019. DOI: 10.5281/ZENODO.2545611
38. Wood species recognition through multidimensional texture analysis / [P. Barmpoutis, K. Dimitropoulos, I. Barboutis et al.] // Computers and Electronics in Agriculture. – 2018. – Vol. 144. – P. 241–248. DOI: 10.1016/j.compag.2017.12.011

DOI 10.15588/1607-3274-2026-2-11